Quantum Electronics **35** (1) 38 – 42 (2005)

PACS numbers: 52.50.Jm; 52.38.Kd; 42.65.Re
DOI: 10.1070/QE2005v035n01ABEH002892

Efficient heating of near-surface plasmas with femtosecond laser pulses stimulated by nanoscale inhomogeneities

Yu.M. Mikhailova, V.T. Platonenko, A.B. Savel'ev

***Abstract*. The interaction of intense ($10^{16} - 10^{18}$ W cm^{-2}) ultrashort (50 – 200 fs) laser pulses with the dense plasmas produced at the surfaces of the porous target is numerically simulated by the particle-in-cell technique. Nanostructure-enhanced absorption of femtosecond pulses in high-porous ($P > 4$) targets is demonstrated. We show that the presence of plasma inhomogeneities essentially alters the heating of plasma electrons and ions; in particular, it stimulates the significant increase in the mean energy and number of hot electrons. The numerical investigation of the dynamics of plasma electrons made it possible to reveal the physical mechanisms behind their heating in a porous medium.**

Keywords: *femtosecond pulses, laser-produced plasmas, nanostructured targets.*

1. Introduction

High-temperature solid-density plasma produced at a target surface by femtosecond laser pulses is now the object of intensive experimental investigations aimed at developing the effective and compact sources of ultrashort X-ray pulses and fast electrons. Recently, the trend has naturally been toward the use of solid targets providing the maximum X-ray yield, the shortest X-ray pulse durations, and the highest energies of fast particles. The key problem in this applied research is the heating of near-surface plasmas up to high temperatures. At the laser-pulse intensities above 10^{15} W cm^{-2} (and below 10^{18} W cm^{-2}) most of the incident laser-pulse energy is reflected from the high-density plasmas (due to the high electric conductivity). At the same time, as the electron temperature grows, the thermal conductivity of plasma increases, thus also severely restricting the heating of plasma particles. An essential improvement of the efficiency of plasma heating can be achieved by using modified solid targets with structured near-surface layers.

Yu.M. Mikhailova, V.T. Platonenko Department of Physics, M.V. Lomonosov Moscow State University, 119992 Moscow, Russia; e-mail: mikhailova@ati.phys.msu.ru;
A.B. Savel'ev International Teaching and Research Laser Center, M.V. Lomonosov Moscow State University, Vorob'evy gory, 119992 Moscow, Russia

Received 30 September 2004
Kvantovaya Elektronika **35** (1) 38 – 42 (2005)
Translated by Yu.M. Mikhailova

Structured targets such as the colloidal metal films [1 – 3], metal nanohole arrays [4, 5], and porous materials (usually, porous silicon) [6, 7] constitute one of the most promising types of targets providing optimal characteristics of near-surface plasmas. As regards porous materials, the properties of plasmas generated at their surfaces essentially depend on the material porosity P (the porosity is generally determined as the ratio of the solid density to the mean density of the porous layer). The increase in the soft X-ray yield from the low-porosity targets ($P \sim 2 - 3$, the porosity is caused by the presence of submicron channels in the silicon single crystal) was first demonstrated in [8], wherein the formation of the low density preplasma layer by the prepulse was shown to be the determining factor.

A more promising material is high-porosity silicon, possessing $P \sim 4 - 7$. Highly porous silicon targets consist of the nano-structured sponge-like layer on the silicon single crystal surface with the mean cluster size varying from 10 to 2 – 3 nm. As it was for the first time shown by the authors of [9], the efficiency of the hard X-ray emission from highly porous samples exposed to femtosecond laser pulses is substantially higher than that from plasmas generated on uniform targets. Besides, both the number and the mean energy of hot electrons are significantly increased when using highly porous targets. The lowering of the contrast of the laser pulse leads in this case to the vanishing of the effect.

The experimentally observed increase in the efficiency of femtosecond-pulse absorption in porous samples has no satisfactory theoretical explanation as yet. The analytic description of the interaction of ultrashort laser pulses with spatially inhomogeneous media, seems to be very complex and had not yet been performed. At the same time, the numerical methods have proved to be powerful in this context. In this work, by means of numerical simulations we have studied the interaction of femtosecond pulses with solid-density plasmas and the influence of target nanostructuring on the efficiency of near-surface plasma heating. Our numerical research is based on the particle-in-cell (PIC) technique supplemented with the procedures simulating Coulomb collisions of plasma particles, which is particularly important at moderate (below 10^{17} W cm^{-2}) intensities of incident light.

2. PIC simulation technique

The approach used in this work rests on the PIC method that is commonly used to simulate the complex processes of nonlinear interaction of light with the laser plasma [10].

This technique is based on the numerical integration of the exact Maxwell equations in the vacuum and relativistic equations of the particle motion. In order to solve Maxwell equations we used an FDTD (finite difference time domain) technique [11], which provides the second-order of accuracy of the time- and space-integration of fields. Ideally, the boundary conditions ensure the transmission of the electromagnetic fields through the boundaries of simulation domain, however, in the case of large angles of incidence of light it is difficult to realize the absolute transmission, and the simulation domain needs to be enlarged. Since the pulse intensity considered in simulations reaches 10^{18} W cm^{-2}, thus entering the regime of the so-called relativistic intensities, the equations of particle motion, integrated in each elementary cycle of calculations, are relativistic.

Boundary conditions for particles imply elastic reflection from the boundaries of the simulation box. We have supplemented the fundamentally collisionless PIC algorithm with the procedures simulating close-range interactions of particles: the electron – ion and ion – ion collisions. This part of numerical calculations is very important for our studies, inasmuch as one of the main mechanisms of absorption of femtosecond pulses with intensities below 10^{17} W cm^{-2} in solid-density plasmas implies electron – ion collisions (the inverse bremsstrahlung). Moreover, as is shown in [12], even at higher laser intensities the collisions are important for the plasma expansion and ion acceleration.

Briefly stated, the procedure of the collision modelling is as follows. Each time step, we directly simulate the interaction of particles within the bounds of each computational cell. Particles are randomly arranged in pairs, for each pair we calculate the stochastic scattering angle, and then find particle momenta. In the case of a small-angle scattering, the rate of change of the mean-square angle of electron – ion scattering is determined as

$$\frac{\mathrm{d}\langle\theta^2\rangle}{\mathrm{d}t} = 2V\sigma(V)N_\mathrm{i},$$

where

$$\sigma(V) = 2\pi\left(\frac{Ze^2}{pV}\right)^2 \ln\Lambda$$

is the electron – ion scattering cross section; V is the relative velocity of colliding particles; p is the momentum; Ze is the ion charge; N_i is the ion density; and $\ln\Lambda$ is the Coulomb logarithm. Assuming that the probability of a particle to be scattered within the angle interval from θ to $\theta + \mathrm{d}\theta$ at the time interval Δt is a Gaussian function with the mean-square angle

$$\frac{1}{2}\langle\theta^2\rangle = 2\pi\frac{Z^2e^2N_\mathrm{i}}{p^2V}\Delta t\ln\Lambda,$$

one can find the stochastic scattering angle for each pair of particles [12]:

$$\theta = \left[-2\langle\theta^2\rangle\ln(1-\xi)\right]^{1/2},$$

where ξ is one of uniformly distributed random numbers ranging from 0 to 1 ($\xi \in [0,1]$). Thus, at each time step we simulate Coulomb collisions of particles, located within the bounds of each computational cell, in such a way that the stochastic scattering angle depends on the velocities, charges and concentration of colliding particles.

The numerical simulation is performed within the framework of the two-dimensional 2D3P technique (particles move in two spatial dimensions, while their momenta and electromagnetic field have all three components). We consider the interaction of 20 – 200-fs laser pulses of intensities $I = 10^{16} - 10^{17}$ W cm^{-2} (linearly polarised radiation, $\lambda = 600$ nm) with the plasma with the steep density profile. A thin slab of the plasma lies in the yz plane, radiation is directed along z axis (Fig. 1). The electric vector lies in the target plane (yz) and has a Gaussian time profile:

$$\boldsymbol{E}(y,z,t) = \boldsymbol{E}(y)\exp\left[-\frac{(t-t_0-z/c)^2}{2\tau^2}\right]\sin\left[\omega(t-z/c)\right].$$

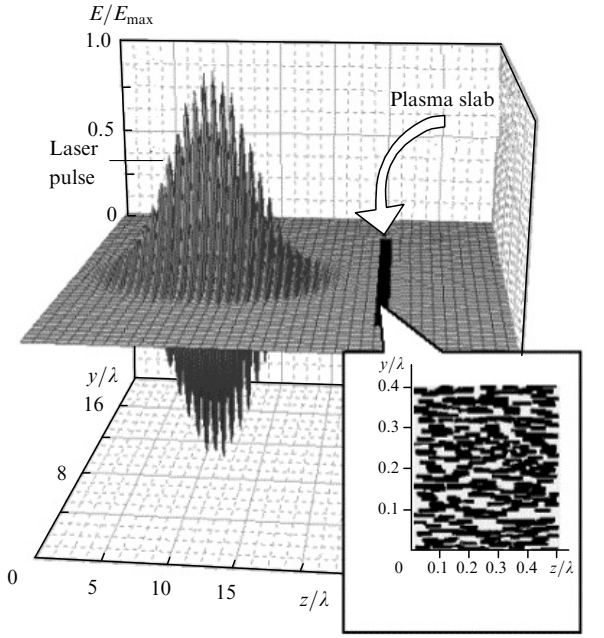

Figure 1. Scheme of the simulation box. The inset shows the example of the simulated porous structure.

The plasma is presumed to be initially ionised; the charge-to-mass ratio is identical for all the ions; the degree of ionisation Z (corresponding to silicon) is assigned depending on the laser-pulse intensity and does not change through the simulation process; the ratio of the ion mass (Si) to the electron mass is 28×1836. Initial electron momenta are assigned using the Maxwellian distribution with the temperature of 10 eV, ions are considered to be cold at starting point.

The plasma with the nanoscale inhomogeneities, which are of main interest in our study, consists of nanometer-sized solid-density fragments (clusters) separated by voids. Sizes of clusters are varied from 10 to 150 nm, the porosity is changed from zero to 8, the initial local density of the plasma $n = (60 - 200)n_\mathrm{c}$, where n_c is the critical plasma density ($n_\mathrm{c} = 3.1 \times 10^{21}$ cm^{-3} for the specified laser wavelength $\lambda = 600$ nm). Unfortunately, for the specified cell of the spatial grid (which is assigned reasoning from the available computational capability as well as from the

requirement of the absence of self-heating of quasiparticles) the realised calculation technique imposes limitation on the minimal size of the plasma cluster – not smaller than 10 nm. This restriction does not allow an accurate simulation of the real experiment with high-porosity silicon. Nevertheless, our calculation has shown that the variation of the cluster size within the range of 10 – 50 nm in case of the fixed porosity virtually does not change the plasma properties (the absorption coefficient, hot-electron temperature). At the same time, the variation of the porosity in case of the fixed cluster size strongly influences the plasma heating. Therefore, the behaviour of plasmas revealed in our studies remains valid even for the smaller sizes of inhomogeneities corresponding to the real highly porous silicon.

The series of tests performed for the moderate intensities of the incident pulse $I \sim 10^{14}$ W cm^{-2}, at which the increase in the plasma temperature and, consequently, the change of the collision frequency in the process of laser-plasma interaction were comparatively slow, have demonstrated a good agreement of the simulation results with the analytic Fresnel formulae.

3. Results and discussion

Although our numerical model cannot lay claim to comprehensive treatment due to its two-dimensional geometry and limitation on the discretisation step, it allowed us to correctly describe the complex process of interaction of high-temperature solid-density plasmas with the strong field of the short laser pulse. Our numerical research has shown that the absorption of the energy of laser pulses with $10^{16} - 10^{17}$-W cm^{-2} intensities in homogeneous plasmas is low (not higher than 20 % in the case of obliquely incident p-polarised light) even when the collisionless mechanisms (such as the vacuum heating) start to contribute to the absorption. At the same time, when a number of nanoscale voids and inhomogeneities are introduced into the plasma, a considerable increase in the absorption coefficient of femtosecond-pulse energy is observed. Figure 2a shows the absorption coefficient of a 200-fs, 2×10^{16}-W cm^{-2} pulse in the homogeneous and nanoporous plasma as a function of the incident angle. The local density, porosity and characteristic size of the cluster of the inhomogeneous plasma are $n = 90n_c$, $P = 5$, $r \sim 30$ nm, respectively. As is seen, for the nanostructured target the absorption of normally incident light is approximately three times higher than that in the case of homogeneous target. The maximum absorption coefficient of the p-polarised wave is more than two times greater in the nanostructured target than in the homogeneous one. The absorption maximum is wider in porous plasma and shifted to smaller incident angles. As is clear from Fig. 2a, in the presence of nanometer-sized plasma inhomogeneities the sensitivity of the absorption to the polarisation of incident light is significantly reduced (the curves corresponding to s- and p-polarised waves are quite close to each other). The lowering of the mean plasma density, which springs from the presence of voids, leads to the decrease in the reflectivity and heat capacity of the plasma as well as to the possibility of the resonant excitation of plasmons at the double laser frequency (i.e. in the regions where the plasma density $n \approx 4n_c$). This fact results in the increase in the absorption coefficient in the plasma with nanoscale inhomogeneities. Figure 2b shows the absorption coefficient

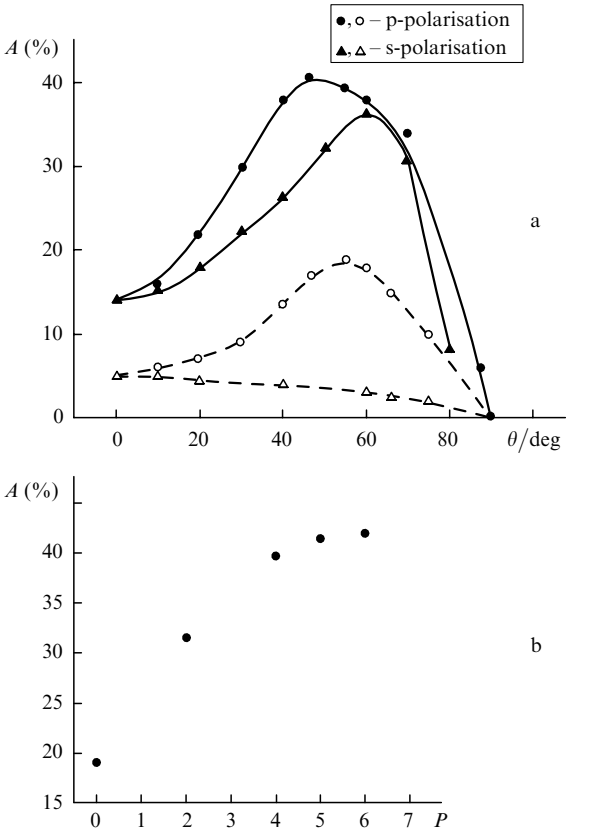

Figure 2. Absorption coefficient A of the energy of the pulse ($\tau = 200$ fs, $I = 2 \times 10^{16}$ W cm^{-2}) of p- and s-polarised light in the inhomogeneous (dark circles) and homogeneous (white circles) plasmas ($n = 90n_c$, $P = 5$, $r \sim 30$ nm) versus the angle of incidence θ (a); and absorption coefficient of the pulse ($I = 10^{16}$ W cm^{-2}, $\tau = 300$ fs, $\theta = 47^\circ$) versus the porosity P for the cluster sizes $r_y = 40$ nm and $r_z = 40$ nm (b).

of the laser pulse ($I = 10^{16}$ W cm^{-2}, $\tau = 300$ fs, $\theta = 47^\circ$), found in the numerical simulation, as a function of the porosity.

The numerical simulation reveals that the generation of hot electrons in the plasma at the surface of the nanostructured target turns out to be more efficient as compared to the case of homogeneous plasmas. Figure 3 shows the energy distributions of plasma electrons after interaction with the laser pulse ($I = 2 \times 10^{16}$ W cm^{-2}). In Fig. 3a, the number of electrons is plotted as a function of the projection of their kinetic energy on the direction perpendicular to the 'average' surface of the target (i.e. the energy corresponding to the momentum p_z). In Fig. 3b, the number of electrons is plotted as a function of the projection of their kinetic energy on the direction parallel to the 'average' surface (i.e. the energy corresponding to the momentum p_y). For comparison, distributions in the case of the homogeneous (solid curve) and inhomogeneous (circles) targets are shown in the same plot. Two different exponential regions can be distinguished in the energy distributions and interpreted as the pieces of the Maxwellian energy distribution with the different effective temperatures. Due to the small number of particles used in the simulation as well as to the strongly nonlinear processes taking place in the plasma, the high-energy tails of distributions suffer strong fluctuations.

As is seen, at low energies we have thermal electrons characterised by the temperatures $T = 550$ and 400 eV in the homogeneous plasma and 900 and 870 eV in the

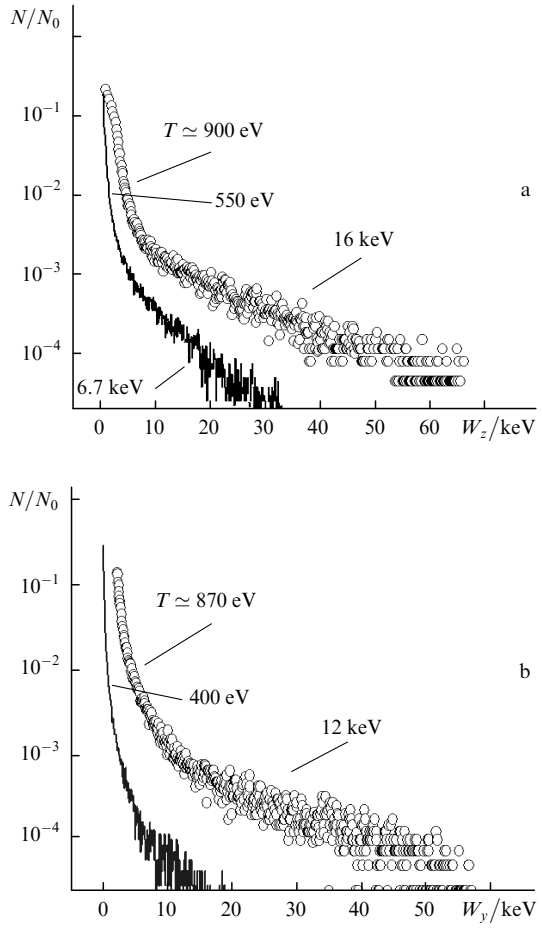

Figure 3. Energy distributions of electrons in directions perpendicular (a) and parallel (b) to the 'average' surface of the porous (circles) and homogeneous (solid curves) targets ($n = 90n_c$, $P = 5$, $r \sim 40$ nm) after the interaction with the laser pulse ($\lambda = 0.6$ μm, $I = 2 \times 10^{16}$ W cm^{-2}, $\tau = 200$ fs, $\theta = 45°$, p-polarisation). The number of electrons N is normalised to their total number N_0.

inhomogeneous plasma. The temperature of hot electrons, corresponding to the high-energy tail, is more than two times greater in the inhomogeneous plasma and reaches 16 and 12 keV against 6.7 keV obtained in the homogeneous plasma. The number of hot electrons in inhomogeneous plasma is approximately three times greater as compared to that of the homogeneous plasma. It is significant that the spatial distributions of hot and thermal electrons are essentially different in uniform and porous plasmas. In the case of homogeneous plasma, the dense region of the plasma contains mainly thermal electrons with only slightly anisotropic energy distribution, hot electrons concentrate in the plasma corona and their energy distribution is strongly anisotropic. In the plasma with nanoscale inhomogeneities both thermal and hot electrons are contained in the high-density plasma and their energy distributions are nearly isotropic.

In order to find an explanation for the enhanced heating of electrons in plasmas with nanoscale inhomogeneities, we consider the dynamics of the electron component, especially the behaviour of an electron in the inhomogeneous electromagnetic field at the pore–matter boundary. We have followed the motion of several quasielectrons in the thin layer near the target surface during the interaction with the femtosecond pulse. The temporal evolution of both the kinetic energy of the test quasielectron and plasma density in the point of its instantaneous location is shown in Fig. 4. As is clearly seen, the test quasielectron suffers an irreversible energy jump at the pore boundary. Considering different pictures of motion of quasielectrons, we have concluded that irreversible energy jumps at the plasma–vacuum boundaries (which become blurred with time) are typical events for fast electrons and happen thanks to the local irregularity of the electric field at the pore boundaries. The efficiency of such irreversible processes that are actually the collisions of electrons with the matter boundaries is directly dependent on the plasma–vacuum surface area. In the nano-structured targets, the plasma–vacuum surface area is significantly enlarged thanks to the well-developed surface and the presence of inner voids. Thus, for example, in highly porous silicon with $P = 5$ the area of the surface of the absorbing layer is increased by a factor of 600. This means that the number of electrons interacting with the nonuniform electromagnetic wave at the plasma–vacuum boundary also grows. Moreover, at the laser pulse intensity $I > 10^{16}$ W cm^{-2} oscillation amplitudes of electrons ($r_{osc} \geqslant 10$ nm) become comparable with the inter-cluster distances ($r_{pore} \sim 10$ nm); the electrons accelerated near the plasma–vacuum boundary as a rule leave their native clusters. This leads to the increase in the effective frequency of collisions of electrons with the matter surface, thus allowing electrons to gain the energy of several kiloelectronvolts.

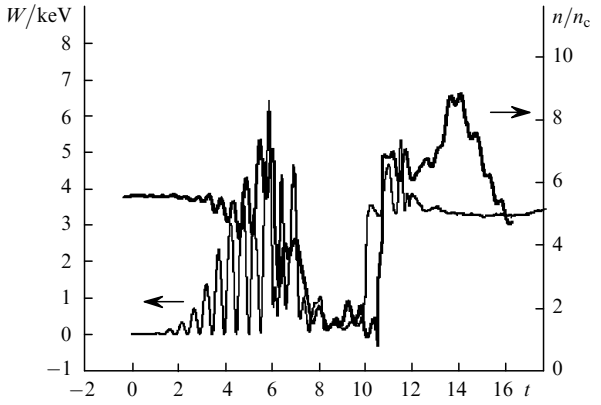

Figure 4. Temporal evolution of the kinetic energy of the test quasielectron and plasma density in the region of its instantaneous location ($I = 5 \times 10^{16}$ W cm^{-2}).

In addition, as we have noticed above, one of the factors, contributing to the increase in the average energy of electrons in the case of the lowered mean density, is the resonant excitation of electron plasma waves at the frequencies close to $2\omega_0$, i.e. in the regions of the plasma with the density about $4n_c$. This resonance, resulting in the resonance of the absorption of the incident radiation energy, is rather wide: for the laser pulse intensity $I = 3.8 \times 10^{17}$ W cm^{-2} and plasma density $n \approx 7n_c$, the absorption coefficient turns out to be just a half of the resonant value.

Thus, the enhancement of the efficiency of heating the plasma at the surface of nano-structured targets (as compared with the heating of homogeneous high-density plasmas of flat targets) is caused by the increase in the

plasma – vacuum boundary as well as the lowering of the mean plasma density.

4. Conclusions

Our numerical investigations allow the conclusion that the efficiency of light absorption in high-temperature solid-density plasmas can be increased by means of the modification of the surface layer of a solid target. Particularly, our calculations have shown that in the case of oblique incidence of femtosecond pulses the absorption coefficient in highly porous nano-structured targets is more than two times greater than that in flat solid targets. The significant peculiarity of the plasma with nano-sized inhomogeneities is the efficient generation of hot electrons: their number in the inhomogeneous plasma is three times greater than that in the homogeneous plasma. Essential differences between flat and structured targets are also observed in the spatial distributions of hot and thermal electrons. In the case of homogeneous plasmas, the dense plasma region contains thermal electrons with slightly anisotropic energy distributions, while hot electrons are situated in the plasma corona and their energy distributions are strongly anisotropic. When applying target nano-structuring, both thermal and hot electrons are contained in the high-density plasma, their energy distributions are nearly isotropic, and their temperatures significantly rise against that of the uniform plasma.

We attribute the effect of the improved heating of femtosecond laser plasmas and efficient generation of hot particles in the nano-structured targets to the lowering of the mean density of the plasma, its thermal and electric conductivity as well as to the significant enlargement of the plasma – vacuum surface area. One of the most important factors determining the increase in the temperature and number of hot electrons is the increase in the effective frequency of irreversible processes of the interaction of fast electrons with the nonuniform electromagnetic field at pore boundaries (i.e. the increase in the frequency of electron collisions with the matter surface).

Acknowledgements. This study was partially supported by the Russian Foundation for Basic Research (Grant Nos 04-02-16341 and 02-02-16563).

References

1. Murnane M.M., Kapteyn H.C., Gordon S.P., Bokor J., Glytsis E.N., Falcone R.W. *Appl. Phys. Lett.*, **62**, 1068 (1993).
2. Gordon S.P., Donnelly T., Sullivan A., et al. *Opt. Lett.*, **19**, 484 (1994).
3. Wulker C., Theobald W., Gnass D.R., et al. *Appl. Phys. Lett.*, **68**, 1338 (1996).
4. Gordienko V.M., Dzhidzhoev M.S., Joukov M.A., et al. *Proc. Conf. 'Superstrong Fields in Plasmas'* (New York: AIP, 1998) Vol. 426, pp 241 – 252.
5. Kulcsar G., AlMawlawi D., Budnik F.W., Herman P.R., Moskovits M., Zhao L., Marjoribanks R.S. *Phys. Rev. Lett.*, **84**, 5149 (2000).
6. Volkov R.V., Gordienko V.M., Dzhidzhoev M.S., et al. *Kvantovaya Elektron.*, **24**, 1114 (1997) [*Quantum Electron.*, **27**, 1081 (1997)].
7. Nishikawa T., Nakano H., Uesugi N., Serikawa T. *Appl. Phys. B*, **66**, 567 (1998).
8. Nishikawa T., Nakano H., Ahn H., Uesugi N. *Appl. Phys. Lett.*, **70**, 1653 (1997).
9. Volkov R.V., Gordienko V.M., Dzhidzhoev M.S., et al. *Kvantovaya Elektron.*, **25**, 5 (1998) [*Quantum Electron.*, **28**, 3 (1998)]; Volkov R.V., Gavrilov S.A., Golishnikov D.M., et al. *Kvantovaya Elektron.*, **31**, 241 (2001) [*Quantum Electron.*, **31**, 241 (2001)].
10. Pukhov A. *Rep. Prog. Phys.*, **66**, 47 (2003).
11. Taflove A., Brodwin M.E. *IEEE Trans. on Microwave Theory & Techn.*, **23**, 623 (1975).
12. Weber S., Bonnaud G., Gauthier J.-C. *Phys. Plasmas*, **8**, 387 (2001).